



EIRENE neutral code modeling of the C-mod divertor

S. Lisgo^{a,*}, P.C. Stangeby^a, C.J. Boswell^b, J.D. Elder^a, B. LaBombard^b,
B. Lipschultz^b, C.S. Pitcher^b, D. Reiter^c, J.L. Terry^b

^a Institute for Aerospace Studies, University of Toronto, 4925 Dufferin Street, Toronto, Canada M3H 5T6

^b MIT Plasma Science and Fusion Center, 175 Albany Street, Cambridge, MA 02139, USA

^c Institute für Plasmaphysik, Forschungszentrum Jülich GmbH, EURATOM Association Trilateral Euregio Cluster,
D-52445 Jülich, Germany

Abstract

The EIRENE Monte-Carlo neutral code is used to calculate neutral pressures throughout the divertor region of the Alcator C-Mod tokamak. A semi-empirical onion-skin method (OSM) is used to calculate the hydrogenic background plasma for a moderate density discharge, $\langle n_e \rangle = 1.5 \times 10^{20} \text{ m}^{-3}$, with a partially detached inner target and an attached outer target. The model parameters are adjusted until there is agreement with the Langmuir probe and spectroscopic data for the divertor region. The measured divertor pressure is 30 mTorr, and for C-Mod divertor dimensions this implies the transition flow regime between free molecular and viscous neutral transport. Therefore, a non-linear BGK-model Boltzmann collision term is included in EIRENE to allow for interactions between neutral particles. For the standard model parameters, the calculated divertor pressure is 7 mTorr. The model parameters are adjusted to reduce the discrepancy, and the plausibility of each variation is discussed.

© 2003 Elsevier Science B.V. All rights reserved.

Keywords: EIRENE; OSM; Divertor; Pressure; Viscosity

1. Introduction

The investigation of neutral production and transport in the divertor can improve our understanding of many issues related to tokamak performance: the effect of neutrals on core confinement modes, impurity compression and codeposition, and pump configuration.

C-Mod is a high B-field tokamak with a compact design: $B_t \sim 8 \text{ T}$, $I_p \sim 1.2 \text{ MA}$, and $R = 0.67 \text{ m}$, $a = 0.21 \text{ m}$. $\langle n_e \rangle$ is typically between 1.0 and $2.5 \times 10^{20} \text{ m}^{-3}$, and measured divertor neutral pressures, p_{div} , range from 1 to 300 mTorr. Initial application of the DEGAS2 [1] and EIRENE [2] Monte-Carlo neutral codes to a moderate

density discharge with $p_{\text{div}} = 30 \text{ mTorr}$ resulted in calculated pressures that were an order of magnitude too low [3,4].

The present work explores possible explanations for the discrepancy by varying the edge plasma solution used with EIRENE. Onion-skin method (OSM) [5] is used to calculate the plasma solution. It is principally an interpretive modeling tool that is used to aid understanding of existing experiments. OSM modeling of the divertor plasma relies extensively on diagnostic data, and has the aim of producing simultaneous agreement with as much of the available data as possible. A necessary condition is that enough data are available to constrain the solution, although no formal criteria for uniqueness have been developed.

The diagnostics used with the OSM are described in Section 2, the details of the OSM solution method are outlined in Section 3, a brief discussion of EIRENE follows in Section 4, and the results and discussion are presented in Section 5.

* Corresponding author. Address: Institute for Aerospace Studies, University of Toronto, 2063 Golden Orchard Trail, Oakville ON L6M 3N5, USA. Tel.: +1-905 469 8599; fax: +1-416 667 7799.

E-mail address: steven@starfire.utias.utoronto.ca (S. Lisgo).

2. Experimental diagnostics

C-Mod shot 990429019 at 950 ms is investigated, which is a D_2 , lower x -point, L-mode discharge, $B \times \nabla B$ towards the divertor, and $\langle n_e \rangle = 1.5 \times 10^{20} \text{ m}^{-3}$. The diagnostics used to constrain the OSM solution are presented in Fig. 1, and the experimental data are plotted along with the modeling results in Section 5. Arrays of ‘domed’ Langmuir probes, LP’s, embedded in the target plates provide measurements of n and T . The probes protrude slightly so that the angle between the magnetic field lines and the probe surface is well defined (greater than 10 degrees) [6]. A toroidally viewing CCD camera is operated with a D_γ filter. Toroidal symmetry is assumed, and a tomographic inversion method is used to generate 2-D D_γ emission profiles in the poloidal plane [7]. The measured ratio of D_α/D_γ (not shown) indicates that these line emissions from the divertor are dominated by volume recombination, and for a recombining plasma the measured Balmer series spectra give n_e from Stark broadening, and T_e from fitting the Saha–Boltzmann distribution to the population densities of the $p = 5$ through $8 \rightarrow 2$ lines [8]. $n_{e,\text{Stark}}$ and $T_{e,\text{Saha}}$ are representative of the recombining regions along the spectrometer viewing chords. p_{div} is measured using a Baratron capacitance manometer gauge located at the bottom of

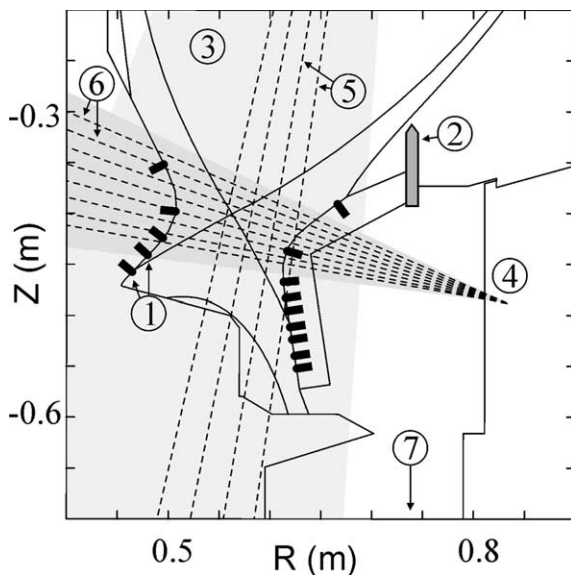


Fig. 1. Poloidal cross-section of the C-Mod divertor showing the available diagnostics: (1) target Langmuir probe arrays, (2) vertical fast reciprocating probe, (3) B_{top} photodiode array (D_α , shaded), (4) K_{bottom} photodiode array (D_α , shaded), (5) K_{top} spectrometer chords, (6) K_{bottom} spectrometer chords, (7) Baratron capacitance manometer pressure gauge. A toroidally viewing CCD camera (not shown) is located at $R = 1.03 \text{ m}$, $Z = -0.16 \text{ m}$.

1.5 m long vertical access port that descends from the floor of the divertor ‘gas box’ chamber.

3. Computer model

OSM is used to calculate the hydrogenic plasma solution in the edge. The magnetic volume is divided into rings along poloidal flux surfaces, and the standard 1-D plasma fluid equations are solved on each ring. Boundary conditions are typically applied from LP measurements of T_e and J_{sat} made at the targets. The OSM solver is iteratively coupled with EIRENE in order to calculate the particle, momentum and energy volumetric source terms related to plasma–neutral interactions. It is assumed that $T_i = T_e$, which may be reasonable for the high density plasmas in C-Mod.

The experimental data indicates that the inner target is weakly detached above the nose, and strongly detached below; see Section 5. Attempts to calculate a stable detached plasma solution using the standard OSM method have been unsuccessful, so the plasma solution along the detachment front is obtained using an empirical, prescription based model. The plasma equations are still solved, but the momentum and energy source terms in the detached region are prescribed so that the T and n profiles are consistent with a simple physical model of detachment [5]. The model parameters are constrained by the experimental data; see Section 5.

4. Neutral transport in EIRENE

The high plasma densities and closed divertor geometry in C-Mod produce high neutral pressures in the divertor. The divertor scale length for C-Mod is approximately 0.3 m, and for typical pressures of $1 < p_{\text{div}} < 100 \text{ mTorr}$ this gives Knudsen numbers in the range $0.01 < Kn < 1$, indicating the transition flow regime. Therefore, interactions between neutral particles should be important and a non-linear BGK-model Boltzmann collision term is included in the EIRENE modeling [9].

5. Results and discussion

For the inner divertor, the sharp decrease in J_{sat} below the inner nose shown in Fig. 2(a) ($0 < \rho < 2 \text{ mm}$) indicates that the plasma is strongly detached. The T_e LP measurements above the inner nose ($\rho > 3 \text{ mm}$) are plotted in Fig. 2(b), and are between 3 and 4 eV, which is inconsistent with $0.65 < T_{e,\text{Saha}} < 0.8 \text{ eV}$ for the same region as shown in Fig. 4(d) (156–161 degrees). Therefore, the LP data for the inner target are disregarded on the assumption that divertor LP’s may be unreliable at

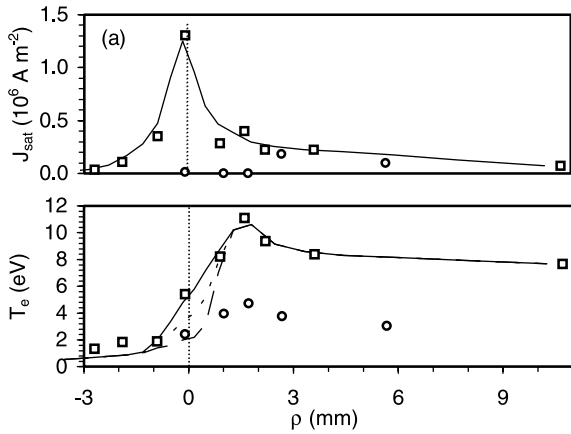


Fig. 2. Measured LP data for the inner (\circ) and outer (\square) divertor region. ρ is the normalized radial coordinate mapped to the outer midplane. (a) J_{sat} – the solid line is the assumed OSM boundary condition at the outer target. (b) T_e – the solid line, short-dashed line and long-dashed line are the boundary conditions assuming $T_{\text{OSP}} = 6.0, 4.0$ and 2.0 eV respectively. The vertical line shows the location of the separatrix. ρ is the distance from the separatrix mapped to the midplane.

very low temperatures (less than ~ 5 eV). The plasma above the inner nose is assumed to be weakly detached, since comparing n_{target} (from J_{sat} and $T_{\text{target}} = T_{e,\text{Saha}}$) with $n_{e,\text{Stark}}$ indicates pressure loss near the targets on the order of 75% of the upstream pressure. There are no target J_{sat} measurements for the inner private flux zone (PFZ) but for modeling purposes the detachment front is assumed to extend along the line of strong D_γ emission from volume recombination, which is often associated with detachment. The front extends through the inner PFZ and SOL; see Fig. 3(a).

The LP data for the outer target are also plotted in Fig. 2, and the higher T_e and J_{sat} values are characteristic

of attached plasmas. The large SOL D_γ emission at the outer nose in Fig. 3(a) may be erroneous because only a single viewing chord of the CCD camera passes through the region. The emission is disregarded since it is not consistent with the outer target LP's, which measure 9 eV at the outer nose ($\rho = 2.5$ mm) and have been validated for $\rho > 2$ mm by comparisons with upstream reciprocating probe data (not shown). In order to reproduce the observed D_γ emission in the outer PFZ, the solution is prescribed for $\rho < -1.1$ mm using the same detachment model employed in the inner PFZ.

p_{div} is a function of neutral production and transport in the divertor, and can be made larger by increasing the neutral source and/or increasing the probability of a neutral reaching the location of the pressure gauge. The OSM plasma solutions can be largely characterized by two parameters: T_{OSP} , the temperature at the outer strike point, which determines the probability of a neutral launched near the OSP entering the PFZ and M_f , the Mach number of the parallel plasma flow into the detachment front, which is a convenient means of scaling the volume recombination source and also provides an additional physical constraint, i.e. that the detached plasma is subsonic [5]. There are no experimental measurements of parallel plasma flow in the inner divertor, so there are no direct constraints on the value of M_f .

Divertor plasmas have been calculated assuming $T_{\text{OSP}} = 2, 4$ and 6 eV, and $M_f = 0.25, 0.5$ and 0.75 . There is no experimental data to exclude the possibility that T_{OSP} is 2 eV, but if T_{OSP} is taken to be less than 2 eV there is significant D_γ emission from the OSP, which is not observed. $T_{\text{OSP}} = 6$ eV is from the LP measurements. The T_{OSP} boundary conditions are modified for $\rho < 2$ mm; see Fig. 2(b). Also, any significant increase in the outer target J_{sat} data results in obvious discrepancies with the reciprocating probe measurements (not shown).

Comparisons between the modeling and the experimental data are presented in Figs. 3–5. Agreement with

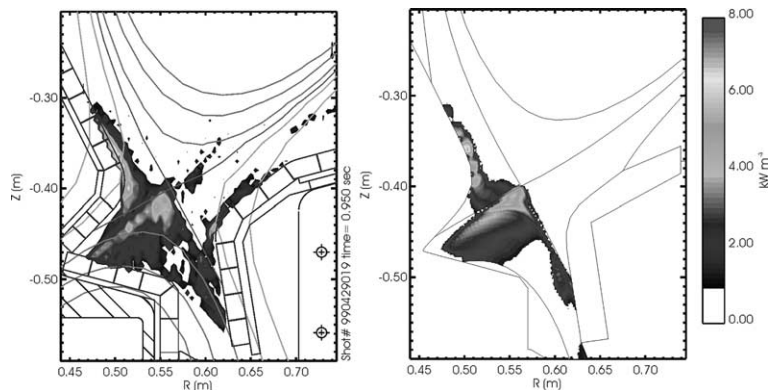


Fig. 3. Poloidal distribution of D_γ emission from the tomographic inversion of the CDD toroidally viewing camera. (a) Experimental data (courtesy of C. Boswell) and (b) calculated emission for $T_{\text{OSP}} = 2$ eV and $M_f = 0.25$.

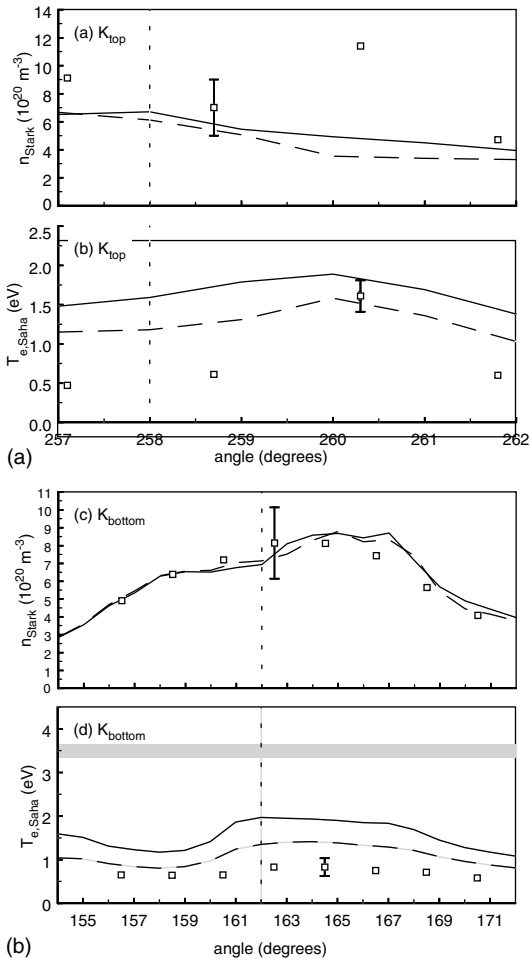


Fig. 4. Analysis of the Balmer series spectra. The open box denotes the experimental data, the solid line is the calculated recombination weighted average of n and T along the spectrometer chords for $M_f = 0.25$, and the dashed line is for $M_f = 0.75$. The calculated values are insensitive to T_{OSP} . (a) $n_{e,Stark}$ for the divertor when viewed from above (K_{top}), (b) $T_{e,Saha}$ viewed from above (K_{top}), (c) $n_{e,Stark}$ viewed from the side (K_{bottom}), and (d) $T_{e,Saha}$ from the side (K_{bottom}). The shaded regions in (d) indicate T_c measured by the LP above the inner nose, which corresponds to $T_{e,Saha}$ data for 156–161 degrees. The vertical dotted lines indicate the location of the divertor x -point.

experiment is generally within uncertainties, with the notable exception of $T_{e,Saha}$, although agreement improves for larger M_f . However, comparisons with $T_{e,Saha}$ are almost certainly affected by the opacity of the plasma to Ly, α photons [10], which is not included in the modeling. A more recent version of EIRENE, which includes photon transport [11], will be employed in the near future. The best match to the D_γ and D_α data is for $T_{OSP} = 2$ eV and $M_f = 0.25$, although line emissions for $M_f = 0.75$ may be in agreement if uncertainties in the

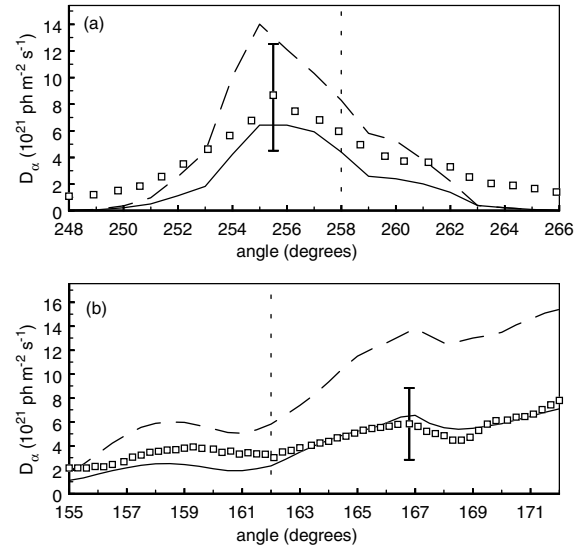


Fig. 5. D_α photodiode measurements for (a) B_{top} and (b) K_{bottom} . The open box's are the experimental data, the solid line is for $M_f = 0.25$, and the dashed line is for $M_f = 0.75$. The emission peaks are insensitive to T_{OSP} . The vertical dotted line indicates the location of the divertor x -point. D_α emissions for angles less than 251 degrees and greater than 263 degrees are thought to be due to reflections and/or ion recycling outside the divertor.

line emission rates used in the modeling are included (under review).

The measured value of p_{div} for this discharge is 30 mTorr, and the calculated values are plotted in Fig. 6. The contributions to p_{div} from volume recombination, predominately from the PFZ, are 30% and 50% for $M_f = 0.25$ and 0.75, respectively. Neutrals recycling from the outer target make up the balance (contributions from recycling and volume recombination above the inner nose are negligible).

Neutral viscosity increases p_{div} by 50% at 7 mTorr ($p_{div,linear} = 4.5$ mTorr), and by 80% at 17 mTorr ($p_{div,linear} = 9.5$ mTorr), which verifies the necessity of including neutral–neutral interactions in the model.

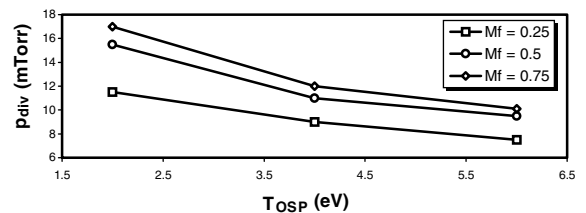


Fig. 6. The calculated divertor pressure. The measured neutral pressure is 30 mTorr.

Despite the higher calculated p_{div} , as compared to the previous neutral modeling efforts, there is still a significant difference between the measured and calculated values. Explanations being investigated include inaccuracies in the collision or line emission rates used with EIRENE, and the possibility of significant ion fluxes to the divertor floor, although there are currently no diagnostics available that could verify the existence of such fluxes.

6. Conclusions

Detailed modeling of the C-Mod divertor plasma using a prescription based OSM solver coupled to the EIRENE neutral hydrogen code has resulted in a calculated p_{div} that agrees with the measured pressure to within a factor of ~ 2 . Neutral viscosity is found to contribute significantly to the p_{div} . Comparisons between the calculated and measured p_{div} suggest that the plasma temperature at the outer strike point is significantly lower, by a factor of ~ 3 , than the 6 eV temperature measured by the target Langmuir probes.

Acknowledgements

Work supported by the US Department of Energy under Contract no. DE-AC02-78ET51013, by IPP Jue-

lich, Germany, and by the Natural Sciences and Engineering Research Council of Canada.

References

- [1] D.P. Stotler, C.F.F. Karney, *Contrib. Plasma Phys.* 34 (1994) 392.
- [2] D. Reiter et al., *Plasma Phys. Contrib. Fus.* 33 (13) (1991) 1579.
- [3] D.P. Stotler, C.S. Pitcher, C.J. Boswell, T.K. Chung, B. LaBombard, B. Lipschultz, J.L. Terry, R.J. Kanzleiter, *J. Nucl. Mater.* 290–293 (2001) 967.
- [4] D. Elder, S. Lisgo, et al., 2000 APS meeting poster presentation.
- [5] P.C. Stangeby, *The Plasma Boundary of Magnetic Fusion Devices*, IOP, Bristol, 2000.
- [6] G.F. Matthews, S.J. Fielding, G.M. McCracken, C.S. Pitcher, P.C. Stangeby, M. Ulrickson, *Plasma Phys. Control. Fusion* 32 (1990) 1301.
- [7] C.J. Boswell, J.L. Terry, B. LaBombard, B. Lipschultz, J.A. Goetz, *J. Nucl. Mater.* 290–293 (2001) 556.
- [8] B. Lipschultz, J.L. Terry, C. Boswell, A. Hubbard, B. Labombard, D.A. Pappas, *Phys. Rev. Lett.* 81 (1998) 1007.
- [9] D. Reiter, Chr. May, M. Baelmans, P. Börner, *J. Nucl. Mater.* 241–243 (1997) 342.
- [10] J.L. Terry, B. Lipschultz, A.Yu. Pigarov, S.I. Krashennikov, B. LaBombard, D. Lumma, H. Ohkawa, D. Pappas, M. Umansky, *Phys. Plasmas* 5 (5) (1998) 1759.
- [11] M. Reiter, S. Wiesen, M. Born, these Proceedings.